Japanese Journal of
Applied Physics

LETTER • **OPEN ACCESS**

Enhancement of a transport critical current by flux trapping in Sn-Pb superconducting solder wire

OPEN ACCESS

Japanese Journal of Applied Physics **65**, 100904 (2026) **LETTER**

https://doi.org/**10.35848/1347-4065/ae6ea6**

Enhancement of a transport critical current by flux trapping in Sn-Pb superconducting solder wire

Takumi Ichikawa[1], Gen Nishijima[2], Yuya Hattori[1], and Yoshikazu Mizuguchi[1*]

[1]*Department of Physics, Tokyo Metropolitan University, Hachioji, Tokyo 192-0397, Japan*
[2]*National Institute for Materials Science, Tsukuba, Ibaraki 305-0003, Japan*

[*]E-mail: mizugu@tmu.ac.jp

Received March 18, 2026; revised April 18, 2026; accepted May 14, 2026; published online May 27, 2026

We investigate the magnetic-field hysteresis effect on a critical current (I_c) of Sn-Pb solders by focusing on flux trapping states. A clear difference in I_c is observed between the zero-field-cooled (ZFC) and field-cooled (FC) states. The I_c for the FC sample is 127.7 A which is larger than I_c = 107.8 A for the ZFC sample at H = 300 Oe. Through investigation of I_c and magnetization, we propose that the phase-separated superconducting alloys can show clearly enhanced I_c by flux trapping, and the exotic states are potentially available for designing superconducting applications. © 2026 The Author(s). Published on behalf of The Japan Society of Applied Physics by IOP Publishing Ltd

A critical current (I_c) is the maximum current that a superconductor can carry while maintaining its superconducting state. I_c improvement of practical superconductors has been an important research objective for a long time.[1–5)] However, recently, nonreciprocal I_c characteristics have been of interest as superconducting diode effect.[6–9)] Furthermore, I_c can be essential for memory-device applications using superconductivity.[10)] To accommodate these emerging applications, further development of techniques for controlling and modifying I_c characteristics is necessary. In this work, we examine magnetic-field (H) sensitivity to transport I_c of well-known phase-separated superconducting alloys, Sn-Pb solders.

The Sn-Pb solders are phase-separated alloys with Sn and Pb microstructures, and magnetic fluxes are trapped after field experience.[11–14)] Using the flux-trapping states below the transition temperature (T_c), nonvolatility of magneto-thermal switching is achieved.[13,15)] In particular, a larger field is trapped in Sn-poor concentrations including a Sn10-Pb90 solder, which is the studied material of this work. The lower-T_c Sn regions are surrounded by the higher-T_c Pb regions, and magnetic fluxes are strongly trapped in the Sn regions by the supercurrents in the Pb regions. In our previous study, the effects of flux-trapped Sn-Pb solders on low-temperature electrical and specific heat measurements have been discussed.[14,16)] The previous studies reported negative effects, such as the broadening of superconducting transition of Sn wire due to flux trapped in Sn-Pb solder joints. In contrast, in this study, we explore positive utilization of the flux-trapping states of Sn-Pb solders to develop superconducting applications. Here, we demonstrate that the I_c of Sn-Pb solders can be tuned by flux-trapping amount, which will be useful for developing superconducting diodes or memory devices based on new strategy.

We used a Sn10-Pb90 (wt.%) round solder wire with a diameter of 1.65 mm (Sasaki Solder Industry). The transport I_c was measured using a standard four-probe method [Fig. 1(a)]. Both ends of the solder wire were mechanically fixed to the current terminals.[17)] The voltage taps were bonded using silver paste and protected with adhesive tape. The distance between the voltage taps was about 3.0 cm. To avoid deformation of the sample wire due to Lorentz force, it was fixed to the sample holder with glass cloth adhesive tape. The applied external magnetic field (H) was perpendicular to the current flow (sample length direction). The measurements were performed in liquid He, and the I_c was evaluated using a criterion of 1.0 μV, which corresponds to 0.33 μV cm^{-1}. The primary purpose of this study was the clarification of the effect of flux trapping [see Fig. 1(b)] on the transport I_c properties.[13–16)] Therefore, we compared the data measured after field cooling (FC, after flux trapping) and zero-field cooling (ZFC). To achieve ZFC states, the sample was heated to T > 10 K, which is higher than T_c = 7.2 K, at H = 0 and cooled to 4.2 K. For the FC data, the sample was cooled at H = 3000 Oe or the field of H = 3000 Oe was applied at T = 4.2 K, where the same flux-trapping states can be obtained. After ZFC or FC processes, the H was fixed to the target fields (H = 300, 400, 500, and 600 Oe). For H below 200 Oe, I_c was not measured because an abrupt sample quench caused a discontinuous voltage jump far beyond the 1.0 μV criterion, making it impossible to identify the I_c.

Figure 1(c) shows the current dependence of voltage (V-I) of the Sn10-Pb90 solder wire measured at T = 4.2 K. The red and blue symbols represent the data taken for the FC and ZFC states, respectively. Noticeably, at H = 300 and 400 Oe, the FC and ZFC data exhibit clear differences, while the FC and ZFC data at H > 400 Oe are comparable. The FC sample (with flux trapping) shows a larger I_c than ZFC. The I_c values determined at 1.0 μV are plotted in Fig. 2 as a function of H. At H = 300 Oe, we obtained I_c = 127.7 A for FC and I_c = 107.8 A for ZFC, resulting in a difference of 19.9 A. Similarly, at H = 400 Oe, the I_c is 68.1 A for FC and 57.8 A for ZFC, showing a difference of 10.3 A. In addition, there is a difference in the sharpness of the transition near the I_c. In the ZFC data, a gradual increase in voltage below I_c is seen, which suggests that the intermediate states are present, and the motion or instability of magnetic flux grows at lower current. In contrast, the FC data shows robustness of the zero-resistivity states up to I_c. The different behavior should be related to the states of the magnetic fluxes.

Figure 3(a) shows the H dependence of magnetization ($4\pi M$) measured after ZFC at T = 4.2 K. A typical hysteresis curve with a critical field of ~ 600 Oe was observed. The

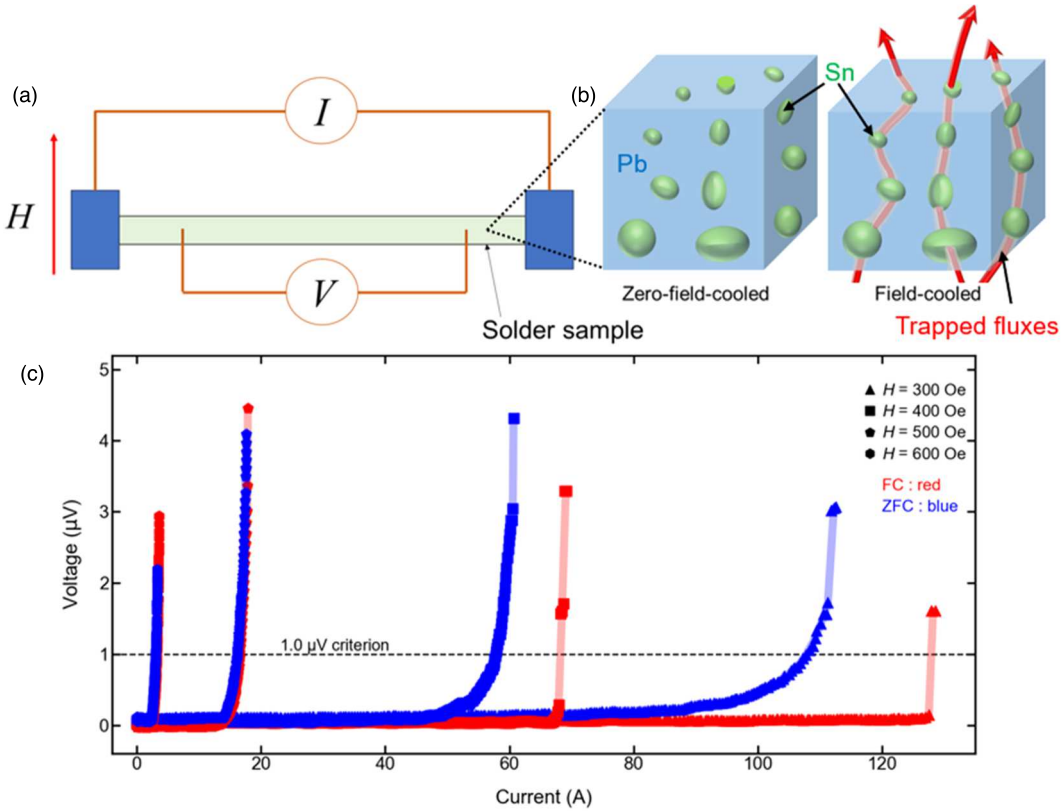

Fig. 1. (a) Configuration of four-terminals method. (b) Schematic images of flux-trapping states (ZFC and FC) of a Sn-Pb solder. (c) Current dependence of voltage.

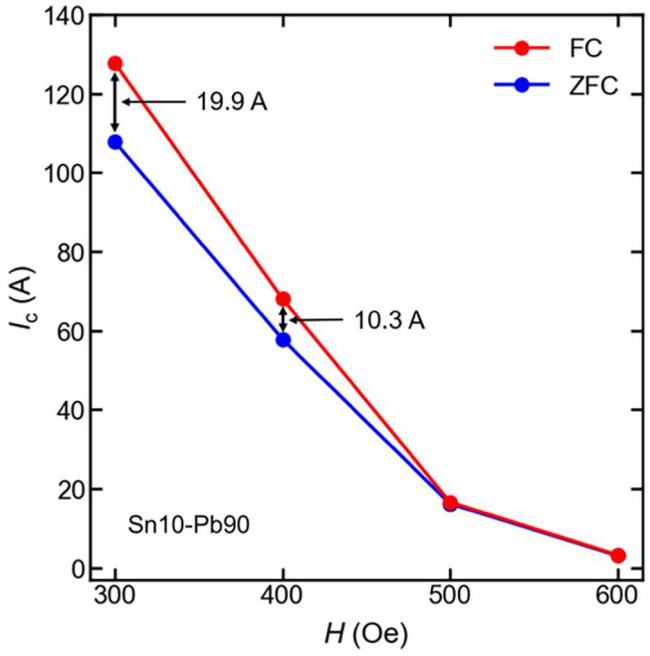

Fig. 2. H dependence of the estimated I_c of the Sn10-Pb90 solder sample.

blue line is the initial magnetization process from $H = 0$ to 3000 Oe after ZFC, corresponding to the ZFC cases. The red line shows the subsequent demagnetizing process from $H = 3000$ Oe to -3000 Oe, which represents the FC (3000 Oe) cases. Black line represents the final upward sweep to $H = 3000$ Oe. Figure 3(b) provides a zoomed view of the middle-field region of Fig. 3(a) to highlight the difference in magnetization profiles between the ZFC and FC cases. The estimated $4\pi M$ and I_c are summarized in Table I.

Figure 4 shows schematic images of flux in the sample interior in each state. In this article, in the state where pinned flux and unstable intermediate-state flux coexist, we specifically define the state of the pinned fluxes as the flux-bound state (FBS). In the FBS, magnetic fluxes are strongly pinned within the Sn regions and protected by the supercurrents in the surrounding Pb regions. Figure 4(a) depicts trapped flux in flux-trapping state. Figure 4(b) illustrates the coexistence of pinned flux in FBS and mobile flux in intermediate state. Figure 4(c) shows flux in intermediate state. Here, we discuss the cause of the difference in I_c at $H = 300$ and 400 Oe between the FC and ZFC cases. As shown in Fig. 3, the initial slope of $4\pi M$ -H up to around 400 Oe shows the Meissner states of a type-I superconductor, which means, at $H = 300$ and 400 Oe, the ZFC sample maintains the Meissner state and behaves like a type-I superconductor. As the applied current increases, the superconducting state is gradually weakened mainly because of self-field generated by the current,[18] and intermediate states are formed near the surface of the wire. The development of surface intermediate states allows magnetic flux to invade by forming large-scale normal-conducting intermediate states as schematically illustrated in Fig. 4(c). These fluxes in Pb regions are typically more unstable and mobile than the vortices strongly pinned in a mixed state. Therefore, the observed broadening of the V-I transitions is related to the formation of the intermediate states and their motion with increasing current. In the FC cases at $H = 300$ and 400 Oe, however, we consider that such formation of large-scale intermediate states does not

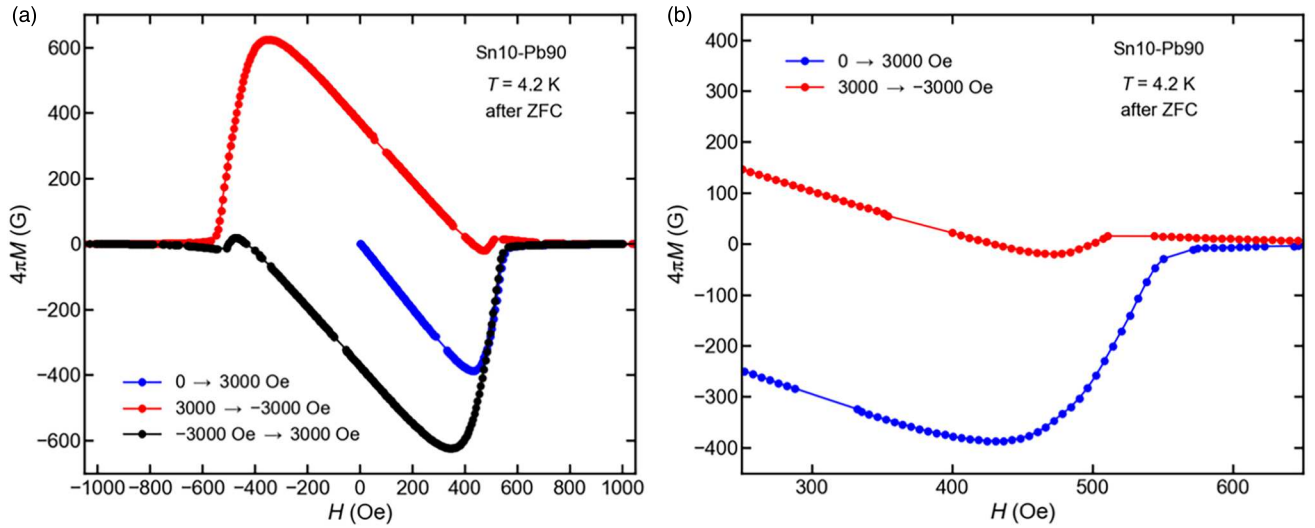

Fig. 3. (a) H dependence of $4\pi M$ of the Sn10-Pb90 solder sample. (b) Zoomed plot at $H = 300$–600 Oe.

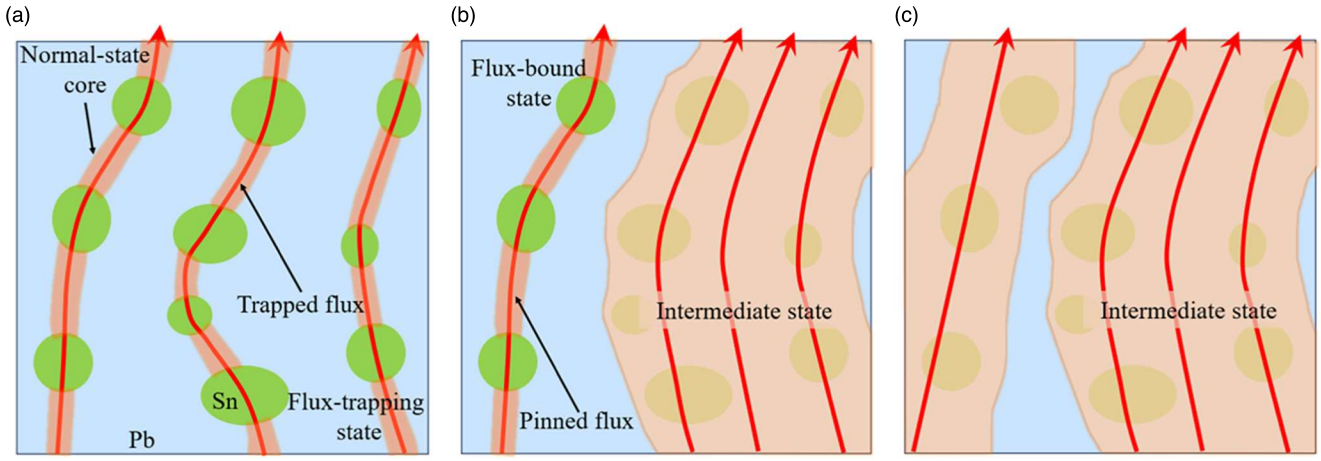

Fig. 4. Schematic image of flux in the sample interior in each state. (a) Trapped flux in flux-trapping state. (b) Coexistence of pinned flux in FBS and mobile flux in intermediate-state. (c) Flux in intermediate-state.

Table I. $4\pi M$ and I_c of the Sn10-Pb90 solder sample at $H = 300$–600 Oe.

H (Oe)	$4\pi M$ (G) (FC)	$4\pi M$ (G) (ZFC)	I_c (A) (FC)	I_c (A) (ZFC)
300	104.4	−294.7	127.7	107.8
400	22.8	−377.9	68.1	57.8
500	1.8	−267.7	16.6	16.2
600	10.0	−6.7	3.2	3.0

occur because of the presence of flux-line routes already-formed by flux trapping as shown in Fig. 4(a). Even with increasing I, the formation of intermediate states would be limited to the outer-core regions. Therefore, I_c is more correlated to the strength of the flux pinning in the FC case. Here, the FC state can be considered similar to a type-II superconductor in that magnetic flux is strongly confined locally. We note that while typical type-II superconductors host vortices with a normal-conducting local core, the fluxes are trapped in the μm-scale Sn regions in the FC state of the Sn10-Pb90 solder.[14)] Although the mechanism of flux (vortex) trapping is different, the relationship between I_c and flux motion should be a common scenario. Namely, the I_c in the FC case is determined by the critical point where the Lorentz force acting on the trapped flux exceeds the pinning force. The convergence of I_c values at $H = 500$ and 600 Oe further supports our scenario. At these higher fields, the ZFC sample is out of the initial Meissner slope, indicating that magnetic flux has already penetrated the sample interior, and the intermediate state has been formed before the current was applied as shown in Fig. 4(c). For the FC case, we assume that the unstable flux in intermediate-state regions coexists with pinned flux in FBS regions before the current application as shown in Fig. 4(b). We estimate the flux-trapping amount is about 400 G at $H = 0$ Oe from Fig. 3. In the flux-trapping process, the internal flux density gradually decreases as H is lowered from H_c of Pb, due to the gradual expulsion of magnetic flux from the sample surface. At lower fields, the intermediate states are reduced because the internal fluxes are mostly pinned in the Sn regions under the protection of the Pb-region supercurrents. In contrast, at higher fields, the internal flux density exceeds the trapping capacity, forcing the excess flux to remain in the Pb regions as unstable and mobile flux in intermediate-state regions. Since intermediate states are established in both the ZFC and FC cases before the current is applied, the V-I curves converge. We remeasured I_c of the same Sn10-Pb90 solder wire and confirmed the reproducibility of the large I_c for the

FC state. $I_c \sim 70$ A was observed at $H = 400$ Oe after FC at 10 kOe.

Reactions of superconducting states to the applied H have been studied in various topics. In superhydride H_3S, strong flux trapping has been reported from field-memory effect on magnetization.[19] Asymmetric field dependence of I_c has also been studied in nano-scale superconducting devices and superconducting tapes.[20–22] Therefore, the sensitivity of I_c to the flux-trapping direction potentially opens new pathways for superconducting applications.

In conclusion, we measured transport I_c of the Sn10-Pb90 superconducting solder wire under magnetic fields after ZFC and FC (flux trapping). For the data at $H = 300$ and 400 Oe, clear differences in I_c and the V-I data were observed between FC and ZFC. The I_c for FC was larger than that for ZFC. The enhancement of I_c and the robustness of the zero-resistivity states with flux-trapping states can be understood by the type-II-like strong flux trapping in the Sn regions in the phase-separated solder. Our results will be useful for further understanding of superconductivity physics of phase-separated alloys and development of exotic superconducting applications using sensitivity of I_c to the magnetic-field direction through the flux-trapping phenomenon.

Acknowledgments The authors thank F. Ando for discussion. This work was partly supported by JST-ERATO (No.: JPMJER2201) and TMU research fund for young scientist.

1) J. Bardeen, Rev. Mod. Phys. **34**, 667 (1962).
2) R. M. Scanlan, A. P. Malozemoff, and D. C. Larbalestier, Proc. IEEE **92**, 1639 (2004).
3) J. L. MacManus-Driscoll and S. C. Wimbush, Nat. Rev. Mater. **6**, 587 (2021).
4) T. Horide and Y. Yoshida, Eur. Phys. J. B **98**, 181 (2025).
5) S. Abdelhaleem, M. O. Alziyadi, A. Alruwaili, M. J. Alawi, A. Alkabsh, and M. S. Shalaby, Appl. Phys. A **131**, 151 (2025).
6) F. Ando, Y. Miyasaka, T. Li, J. Ishizuka, T. Arakawa, Y. Shiota, T. Moriyama, Y. Yanase, and T. Ono, Nature **584**, 373 (2020).
7) M. Nadeem, M. S. Fuhrer, and X. Wang, Nat. Rev. Phys. **5**, 558 (2023).
8) J. Ma, R. Zhan, and X. Lin, Adv. Phys. Res. **4**, 2400180 (2025).
9) U. Nagata, M. Aoki, A. Daido, S. Kasahara, Y. Kasahara, R. Ohshima, Y. Ando, Y. Yanase, Y. Matsuda, and M. Shiraishi, Phys. Rev. Lett. **134**, 236703 (2025).
10) B. Baek, W. H. Rippard, S. P. Benz, S. E. Russek, and P. D. Dresselhaus, Nat. Commun. **5**, 3888 (2014).
11) J. D. Livingston, Phys. Rev. **129**, 1943 (1963).
12) S. Furuya, A. Tominaga, and Y. Narahara, J. Low Temp. Phys. **53**, 477 (1983).
13) H. Arima, M. R. Kasem, H. Sepehri-Amin, F. Ando, K. Uchida, Y. Kinoshita, M. Tokunaga, and Y. Mizuguchi, Commun. Mater. **5**, 34 (2024).
14) Y. Mizuguchi, T. Murakami, M. R. Kasem, and H. Arima, EPL **147**, 36003 (2024).
15) P. Rani, T. Murakami, Y. Watanabe, H. Sepehri-Amin, H. Arima, A. Yamashita, and Y. Mizuguchi, Appl. Phys. Express **18**, 033001 (2025).
16) T. Ichikawa, Y. Watanabe, T. Murakami, P. Rani, A. Yamashita, O. Miura, and Y. Mizuguchi, Jpn. J. Appl. Phys. **63**, 100906 (2024).
17) G. Nishijima, S. Matsumoto, A. Nakai, H. Sakamoto, S. Mukoyama, and Y. Miyoshi, IEEE Trans. Appl. Supercond. **29**, 6602105 (2019).
18) D. Dew-Hughes, Low Temp. Phys. **27**, 713 (2001).
19) V. S. Minkov, V. Ksenofontov, S. L. Bud'ko, E. F. Talantsev, and M. I. Eremets, Nat. Phys. **19**, 1293 (2023).
20) T. Aomine, E. Tanaka, S. Yamasaki, K. Tani, and A. Yonekura, J. Low Temp. Phys. **74**, 263 (1989).
21) K. Ilin, D. Henrich, Y. Luck, Y. Liang, and M. Siegel, Phys. Rev. B **89**, 184511 (2014).
22) N. M. Strickland, S. C. Wimbush, M. W. Rupich, and N. J. Long, IEEE Trans. Appl. Supercond. **29**, 8001304 (2019).